# Numerical Study on Pulsatile Flow of Non-Newtonian Fluid Through Arterial Stenosis

**Mohammad Ali, Kazi Shafi Sami, and Amanullah Kabir Tonmoy**

**Abstract** In this research, the pulsatile blood flow through stenosed artery of 60% severity has been investigated. Flow behavior for two non-Newtonian viscosity models is compared. A standard $k$-$\omega$ turbulence model is used for turbulent flow at post-stenotic region. The Wall Shear Stress (WSS), hydrostatic pressure, and streamline contours at different time steps are obtained. A Fluid Structure Interface (FSI) model is used to determine the dynamic structural behavior with fluid flow. The maximum deformation, maximum von-mises stress, and peak principal stress that are obtained for FSI model. Wall shear stress and von-mises stress are found significantly higher at throat region. Peak principal stress is the highest over time at pre-stenotic region. Streamline patterns are observed for different time steps with the change in inlet velocity.

**Keywords** Non-Newtonian fluid · Fluid structure interface · Wall shear stress

## 1 Introduction

Atherosclerosis is a disease characterized by the formation of plaque. This plaque causes stenosis which is defined as a partial constriction of blood vessel due to accumulation of LDL and fats resulting in this abnormal growth of tissue. When the plaque is formed, the hemodynamic parameters are significantly changed. The change in hemodynamic parameters play a significant role in enlarging the plaque. Eventually, it leads to cardiovascular diseases. Study of blood flow in stenosed artery is important for interpreting the causes and progression of atherosclerosis. Computational fluid dynamics are used to examine the role of hemodynamics on the localization, development, and progression of arterial stenosis. The results of computational simulations obtained by Stroud et al. [1] should supplement MR and other in vivo diagnostic techniques to provide an accurate picture of the hemodynamics in particular vessels.

M. Ali (✉) · K. S. Sami · A. K. Tonmoy
Department of Mechanical Engineering, Bangladesh University of Engineering and Technology, Dhaka 1000, Bangladesh
e-mail: mali@me.buet.ac.bd

Casscell [2] observed that increasing degrees of stenosis carries greater risks of atherothrombotic events. Pasterkamp and Smits [3] found arteries often dilated in an attempt to normalize elevated wall shear stresses as atherosclerosis develops, a process known as expansive remodeling. Manica and Bortoli [4] simulated incompressible non-Newtonian flow through channels with expansion using the power law model. Nakamura and Sawada [5] observed that the non-Newtonian property of blood weakens the distortion of flow pattern, pressure, and shear stress at the wall associated with the stenosis. Johnston and Kilpatrick [6] investigated the Newtonian model of blood viscosity as a good approximation in regions of mid-range to high shear, and they advised to use the generalized power law model (which tends to the Newtonian model in those shear ranges in any case) in order to achieve better approximation of wall shear stress at low shear. Gijsen and Allanic [7] found that the non-Newtonian model could not be predicted with a Newtonian model with a constant viscosity. Ballyk and Steinman [8] studied non-Newtonian blood rheology which creates a significant effect on steady flow wall shear stresses, but no significant effect on unsteady flow wall shear stresses. Li and John [9] observed restraining wall motion due to severe stenosis which results in higher blood velocities and higher peak wall shear stress, and localization of hoop stress. Inzitari et al. [10] found that forty-five percent of strokes in patients with asymptomatic stenosis of 60–90% severity are attributable to lacunar stroke. Below 60% severity, the chances of stroke are less. So, an axisymmetric 3D model artery of 60% severity was considered by Sami and Tonmoy [11]. The total length of the model is taken as 102 mm (17D) where diameter $D = 6$ mm. A parabolic velocity profile with velocity pulse is used as inlet boundary condition. At velocity pulse, Reynolds number varies from 200 to 1100 to observe the effect of fluctuating flowrate. For FSI model, one-way coupling method is used. For one-way Fluid Structure Interface (FSI) model, the artery is assumed to be isotopic linear elastic and Reynolds number varies from 240 to 310.

## 2 Methodology

Numerical simulation is performed by ANSYS Fluent 15.07. Figure 1 shows the shape of the stenosis in the blood vessel which is created by using cosine formula. ANSYS CAD software is used to build the geometry. Discretization of domain is performed in ANSYS mesh module. Pressure-based solver is used. Low Reynold $k$-$\omega$ turbulent model is used for turbulence in post-stenotic region. Simple algorithm
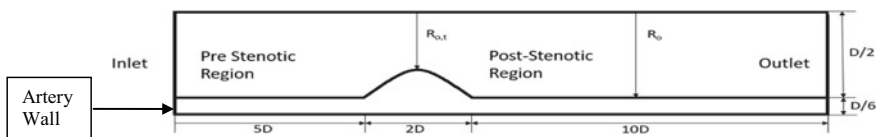


**Fig. 1** Schematic of the geometry

is selected for pressure velocity coupling. First-order upwind scheme is employed as a numerical scheme for discretization of the momentum equation. In ANSYS Workbench, the FSI (one-way coupling) analysis can be performed by connecting the coupling participants to a system component called system coupling. A participant either feeds or receives data in a coupled analysis. Here, ANSYS Fluent (participant 1) and ANSYS Transient Structural (participant 2) are acting as coupling participants. The inlet boundary conditions and viscosity equations are given by C-language code using the interface of User Defined Function (UDF).

## 3 Governing Equations

The following governing equations are used to perform the present numerical study.

**Mass conservation or continuity equation**:

$$\frac{\partial \rho}{\partial t} + \nabla \cdot (\rho v) = 0 \tag{1}$$

**Momentum equation**:

$$\frac{\partial \rho \mathbf{v}}{\partial t} + \nabla \cdot (\rho \mathbf{v}\mathbf{v}) = \nabla \cdot \boldsymbol{\tau} + \rho \mathbf{b} \tag{2}$$

Here, $b$ is the body force. Blood is considered to be a single phase, incompressible, homogeneous non-Newtonian fluid. Here, typical value of density is, $\rho = 1050 \text{ kg/m}^3$. Viscosity of the blood is defined as Carreau and cross model.

**Cross Model**:

$$\mu = \mu_\infty + (\mu_0 - \mu_\infty)\left[1 + \left(\frac{|\dot{\gamma}|}{\gamma_c}\right)^m\right]^{-1} \tag{3}$$

Here, viscosity at zero shear rate, $\mu_0 = 0.0364$ Pa s, viscosity at infinite shear rate, $\mu_\infty = 0.00345$ Pa s, reference shear rate, $\gamma_c = 2.63 \text{ s}^{-1}$ and $m = 1.45$.

**Carreau model**:

$$\mu = \mu_\infty + (\mu_0 - \mu_\infty)\left[1 + (\gamma_c \dot{\gamma})^2\right]^{\frac{n-1}{2}} \tag{4}$$

Here, $\mu_0 = 0.056$ Pa s, $\mu_\infty = 0.00345$ Pa s, $\gamma_c = 3.313 \text{ s}^{-1}$, and $n = 0.3568$. For FSI model, elastic modulus of the artery wall is given 9.1 MPa. Density of artery wall is 1300 kg/m$^3$. Poisson ratio of artery wall is 0.49 [12]. As the pumping action of heart is periodic, so an oscillatory blood flow is sufficient to consider. Womersley
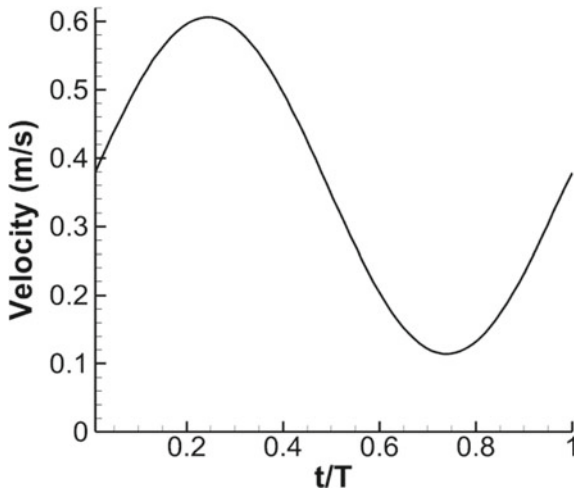
**Fig. 2** Velocity distribution with non-dimensional time ($t/T$) used at inlet

number for this investigation is 4.58. The constant pressure of 75 mm Hg is kept at outlet. Figure 2 shows the velocity pulse at inlet.

## 4 Results and Discussion

The present research is devoted to compare the two different non-Newtonian models and studies the fluid structure interaction between the blood flow and the plaque in a 3D modeled arterial stenosis. The code validation has been done by comparing computational results with the experimental results obtained by Ahmed and Giddens [13]. From experiment, single stenosis with 75% severity model is considered for numerical study. Steady inlet velocity condition is given. Glycerin-water mixture is used as flowing fluid which is modeled as non-Newtonian fluid using power law for validation. Velocity profiles in the post-stenotic regions are compared for $Z = D$, $2.5D$ where $Z$ is the normalized distance from the center of the stenosis. From the comparison in Fig. 3, it can be shown that axial velocity patterns are very much similar to the experimental pattern for $Z = 2.5D$. But due to turbulence model, the numerical result slightly overpredicts near centerline. A grid independence test has been performed to ensure that the numerical solutions are independent on the choice of the grid arrangements between 627,222 and 986,880 elements.

Wall Shear Stress (WSS) is the force on flowing blood on endothelial surface of vessel. As the shear stress for flow varies from zero at the centerline to a maximum at the wall, the wall shear stress becomes an important parameter to determine to flow characteristics. In this research, high wall shear stress is dominant in high flow velocities at throat region. Low shear stress obtained in the descending zone is due to
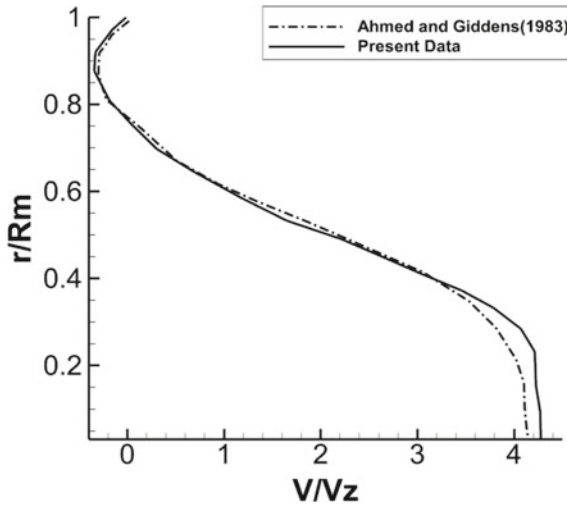
**Fig. 3** Validation with the experimental result. When $Z = 2.5D$ for $Re = 500$

increase in area. For both Carreau and cross viscosity model, Figs. 4, 5, and 6 show that the maximum wall shear occurs at throat in the upper boundary. Here, WSS is higher in cross viscosity model. For both models, the WSS is uniformly distributed at pre-stenotic and post-stenotic region for this geometry.

As the wall shear stress is directly proportional to the pressure drop, hydrostatic pressure is an important parameter to show the effect of stenosis. Figures 7, 8, and 9 show the fluctuation of pressure occurred in different time steps due to the effect of pulsatile velocity at inlet. Due to blockage, large pressure drop is observed at throat. The streamline pattern is changed due to the presence of stenosis. As the flow is sinusoidal and time dependent, significant flow variation on the post-stenotic region
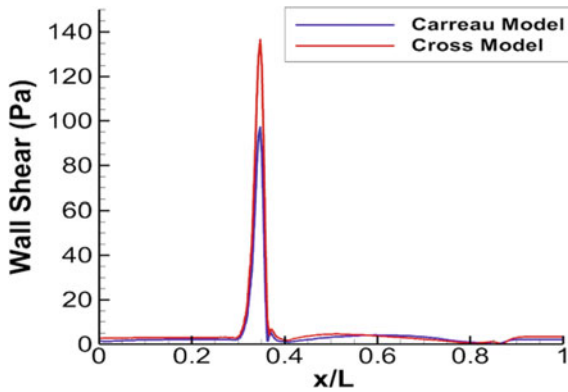


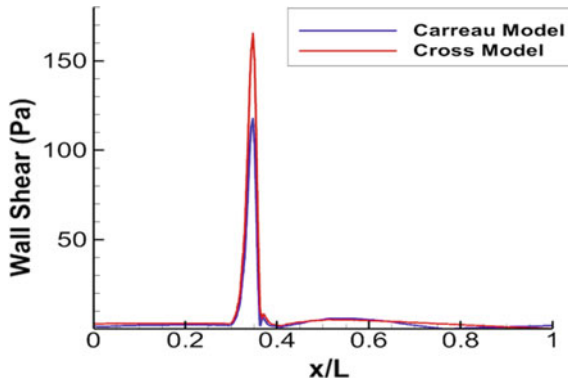**Fig. 4** Wall shear stress distribution at upper wall at $t/T = 0.125$

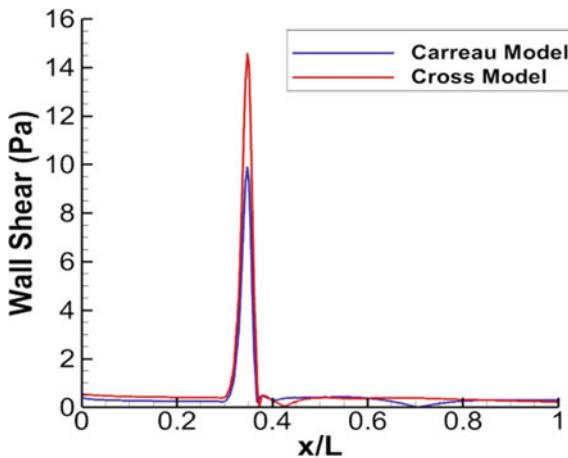**Fig. 5** Wall shear stress distribution at upper wall at $t/T = 0.25$



**Fig. 6** Wall shear stress distribution at upper wall at $t/T = 0.75$

are observed. Variations of streamlines contours have been investigated to study the flow pattern of blood through the stenotic artery. Figure 10 shows streamline contours for Carreau and cross model vortex at three different time steps. At $t/T = 0.125$, two large vortices length of 0.038 and 0.0465 m from the throat of 60% severities presented in Fig. 10 (a, d). At $t/T = 0.25$, two separated vortex, regions are created near the upper wall in Carreau model for 60% severity presented in Fig. 10b. At Fig. 10e, there is a large vortex region of length 0.0498 and 0.0557 m created at upper and lower wall, respectively, in cross model. At $t/T = 0.75$, the massive changes occur. At Fig. 10 (e, f), there are two vortex rings created at pre-stenotic region near the wall, and combination of large and small vortex rings are observed for Carreau model, and a large vortex ring near the upper wall changes the direction
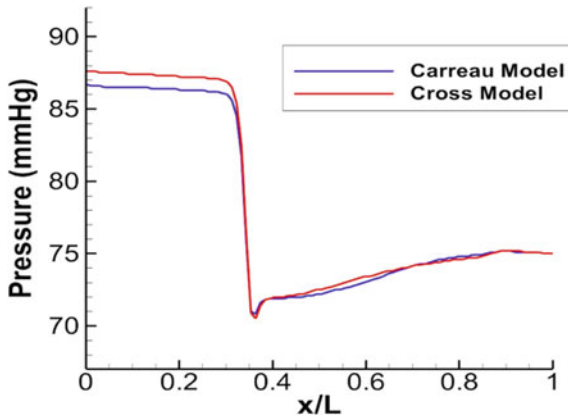
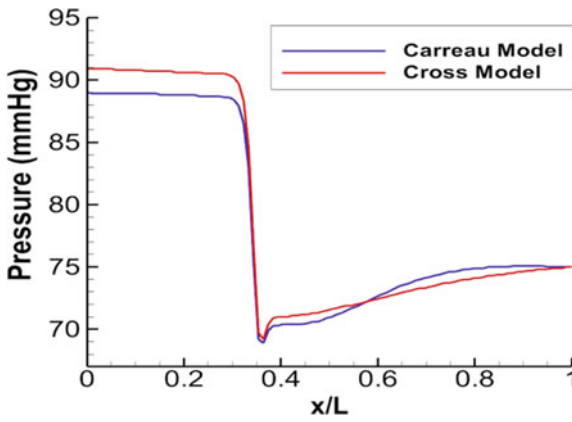**Fig. 7** Centerline pressure distribution at $t/T = 0.125$
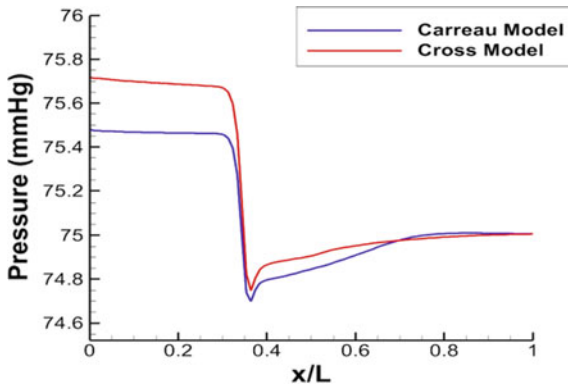
**Fig. 8** Centerline pressure distribution at $t/T = 0.25$

**Fig. 9** Centerline pressure distribution at $t/T = 0.75$

a) t/T=0.125                                                    b) t/T=0.25

c) t/T=0.75                                                    d) t/T=0.125

e) t/T=0.25                                                    f) t/T=0.75
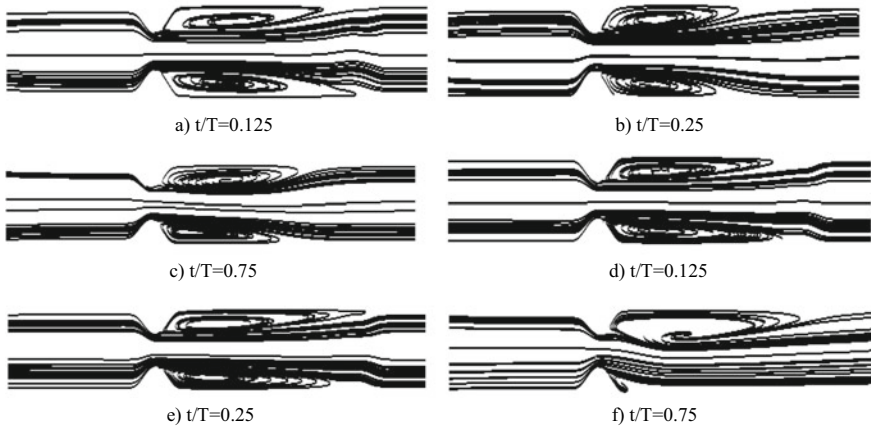
**Fig. 10** Streamline contours at different time steps for Carreau model (**a–c**) and cross model (**d–f**)

of the flow a little for cross model which is unusual. From this observation, Carreau model is more suitable for the fluid structure interface analysis.

Principal stress is one of the most significant parameters in determining the wall rupture. From Fig. 11, the peak principal stress basically occurs when the velocity and pressure gradient are maximum at pre-stenotic region. Figure 13 shows that the total deformation is maximum there at pre-stenotic region because of the high normal stress. Von-mises stress is another vital parameter in determining the risk of rupture. Von-mises stress is the equivalent of uni-axial tensile stress. Figure 12 shows that the von-mises stress is very high at throat region.
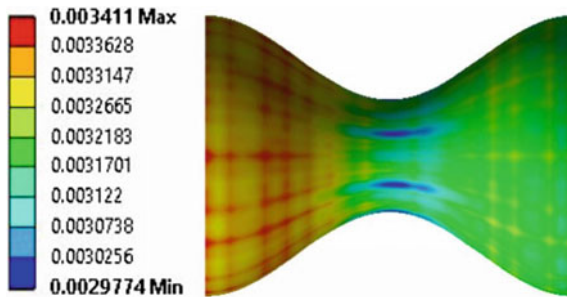


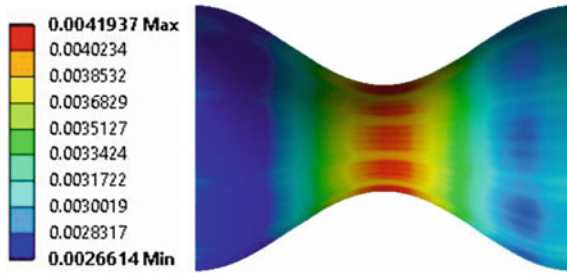**Fig. 11** Maximum principal stress (MPa) over time Figure missing

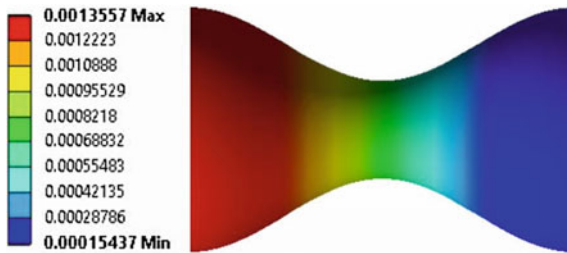**Fig. 12** Maximum von-mises stress (MPa) over time Figure missing



**Fig. 13** Total deformation along *x*-axis (mm) Figure missing

## 5 Conclusion

A numerical investigation is performed here to analyze the effects of stenosis on flow parameters. For this analysis, the high shear stress at throat will cause the possibility to damage the intimal tissue. At throat, there is higher chance of damage of endothelial wall due to shearing action. Low shear stress at post-stenotic region due to recirculation enhances the possibility of plaque formation in post-stenotic region. Vortex length changes as the Reynolds number changes with the velocity pulse at inlet. Centerline pressure distribution is quite similar for Carreau and cross model. In FSI model, deformation is very small. Both peak principal stress and deformation occur at pre-stenotic region due to high hydrostatic pressure gradient and constriction. Better result will be found considering hyper-elastic artery wall by using Mooney–Rivlin Model.

# References

1. Stroud JS, Berger SA, Saloner D (2000) Influence of stenosis morphology on flow through severely stenotic vessels: implications for plaque rupture. J Biomech 33(4):443–455
2. Casscells W, Naghavi M, Willerson JT (2003) Vulnerable atherosclerotic plaque: a multifocal disease. Circulation 107(16):2072–2075
3. Pasterkamp G, Smits PC (2002) Imaging of atherosclerosis. Remodelling of coronary arteries. J Cardiovasc Risk 9(5):229–235
4. Manica R, De BAL (2011) Simulation of incompressible Non-Newtonian flows through channels with sudden expansion using the power-law model. TEMA-Tendencias Matematica Apl Comput 4(3):333–340
5. Nakamura M, Sawada T (1988) Numerical study on the flow of a non-Newtonian fluid through an axisymmetric stenosis. J Biomech 11(2):28–31
6. Johnston PR, Corney S, Kilpatrick D (2004) Non-Newtonian blood flow in human right coronary arteries: steady state simulations. J Biomech 37(5):709–720
7. Gijsen FJH, Allanic E, Van De Vosse FN, Janssen JD (1999) The influence of the non-Newtonian properties of blood on the flow in large arteries: unsteady flow in a 90° curved tube. J Biomech 32(7):705–713
8. Ballyk PD, Steinman DA, Ethier CR (1994) Simulation of non-Newtonian blood flow in an end-to-side anastomosis. Biorheology 31(5):565–586
9. Li MX, Beech-Brandt JJ, John LR, Hoskins PR, Easson WJ (2007) Numerical analysis of pulsatile blood flow and vessel wall mechanics in different degrees of stenoses. J Biomech 40(16):3715–3724
10. Inzitari D, Eliasziw M, Gates P, Sharpe BL, Chan RK, Meldrum HE, Barnett HJ (2000) The causes and risk of stroke in patients with asymptomatic internal-carotid-artery stenosis. North Am Symptomatic Carotid Endarterectomy Trial Collaborators. J Med 342(23):1693–700
11. Sami KS, Tonmoy AK, Characteristics of Non-Newtonian flow through arterial stenosis. B.Sc. Engineering, thesis, Department of Mechanical Engineering, BUET, Bangladesh
12. Jahangiri M, Saghafian M, Sadeghi MR (2015) Numerical study of turbulent pulsatile blood flow through stenosed artery using fluid-solid interaction. Comput Math Methods Med ID 515613, 1–10
13. Ahmed SA, Giddens DP (1983) Flow disturbance measurements through a constricted tube at moderate Reynolds numbers. J Biomech 16(12):955–963